Efficient Fast Multipole Method for low frequency scattering

By Eric Darve

1. Introduction

1.1. *Motivation*

The Fast Multipole Method (FMM) is a numerical method which has found wide acceptance in the scientific community. It is a fast summation method for potentials in $1/r$ and has applications in many areas such as Laplace and Poisson equations, particle simulations, molecular dynamics, etc. Another application of the FMM to Maxwell and Helmholtz equations (kernel in $\exp(\imath\kappa r)/r$) was initiated by Rokhlin (1990). However the derivation of the FMM for Maxwell/Helmholtz has two major drawbacks. First, the method fails when the size of the clusters becomes very small compared to the wavelength. This problem is known as sub-wavelength breakdown. The second limitation is the fact that numerically the approximation error of the method cannot be reduced beyond $\sim 10^{-4}$ relative error even when the number of poles is increased. This is due to numerical instabilities which, when coupled to roundoff errors, lead to a divergence of the method as the number of poles is increased beyond a certain threshold. In particular these two limitations mean that the FMM cannot be used for computations where the distribution of points is highly inhomogeneous (discretization of small details on the surface of the object for example) or when high accuracy is required (because of cavity resonances for example). We have developed a new variant of the FMM with complexity $n \log n$ which is based on plane wave expansions. This new formulation leads to a method which is stable at all frequencies (no sub-wavelength breakdown) and is arbitrarily accurate. This method is more efficient and mathematically simpler than previous methods, such as the ones described in Greengard (1998) or Hu, Chew and Michielssen (1999). It is also more efficient than the traditional FMM for Maxwell/Helmholtz at high frequencies, discussed by Darve (1999) and Engheta (1992). In this article we propose a review of the traditional multipole techniques for potentials in $\exp(\imath\kappa r)/r$ and describe our new technique based on plane wave expansions.

1.2. *Overview of the article*

We start with a general overview of the article where we present the main results and achievements.

We are interested in the application of the Fast Multipole Method (FMM) to Maxwell or Helmholtz equations. When these equations are solved using integral equations, the free-space Green's kernel is defined as:

$$K(\boldsymbol{x},\boldsymbol{y}) = \frac{\exp(\imath\kappa|\boldsymbol{x}-\boldsymbol{y}|)}{|\boldsymbol{x}-\boldsymbol{y}|}$$

This kernel can be approximated using the following expansion:

$$\frac{e^{\imath\kappa|\boldsymbol{x}+\boldsymbol{y}|}}{|\boldsymbol{x}+\boldsymbol{y}|} = \lim_{l\to+\infty} \int_{S^2} e^{\imath\kappa\langle\boldsymbol{\sigma},\boldsymbol{y}\rangle}\, T_{l,\sigma}(\boldsymbol{x})\, d\boldsymbol{\sigma} \tag{1.1}$$

where S^2 is the unit sphere. We denote by $|\bullet|$ the modulus and by $\langle \bullet, \bullet \rangle$ the scalar product. The function $T_{l,\sigma}(\boldsymbol{x})$ is defined by:

$$T_{l,\sigma}(\boldsymbol{x}) = \imath\kappa \sum_{m=0}^{l} \frac{(2m+1)\imath^m}{4\pi} h_m^{(1)}(\kappa|\boldsymbol{x}|) P_m(\cos(\boldsymbol{\sigma}, \boldsymbol{x})) \tag{1.2}$$

where $h_m^{(1)}$ is a spherical Bessel function and P_m is a Legendre polynomial. This expansion has been widely used, in particular by Song *et al.* (1997), Epton & Dembart (1995) and Darve (1999), etc.

This expansion has a major disadvantage, which is the divergence of $h_m^{(1)}(\kappa|\boldsymbol{x}|)$ for $m \to +\infty$ and for $|\boldsymbol{x}| \to 0$: see Eq. (2.1). This leads to two kinds of numerical instabilities. First, when the size of the clusters becomes too small the transfer function $T_{l,\sigma}(\boldsymbol{x})$ starts diverging. This corresponds to a situation where we have a large number of points concentrated in a region of diameter D where $D \ll \lambda$, the wavelength. This is often called the sub-wavelength breakdown. Secondly, to reduce the error ϵ of the method we need to increase l. However when l becomes large compared to $\kappa|\boldsymbol{x}|$, $T_{l,\sigma}(\boldsymbol{x})$ starts diverging. This means that because of strong numerical instabilities we are not able to reduce the error arbitrarily. For practical cases, the error ϵ is bounded below by approximately 10^{-4}.

Our new formulation of the FMM, the Plane Wave Fast Multipole Method (PW-FMM), is based on the following expansion:

$$\frac{e^{\imath\kappa|\boldsymbol{r}|}}{|\boldsymbol{r}|} = \frac{\imath\kappa}{2\pi} \int_{S^{z+}} e^{\imath\kappa\langle\boldsymbol{\sigma},\boldsymbol{r}\rangle}\, d\boldsymbol{\sigma} + \frac{1}{\pi} \int_{\chi=0}^{+\infty} \int_{\phi=0}^{2\pi} e^{-\chi^2 z}\, e^{\imath\sqrt{\chi^4+\kappa^2}(x\cos\phi + y\sin\phi)}\, \chi\, d\chi\, d\phi \tag{1.3}$$

with $\boldsymbol{r} = (x, y, z)$ and S^{z+} is the upper hemisphere (subset of the unit sphere of all points with positive z-coordinate). See Eq. (3.1). These two terms have very simple values in the case $x = y = 0$, $z > 0$:

$$\frac{\imath\kappa}{2\pi} \int_{S^{z+}} e^{\imath\kappa\langle\boldsymbol{\sigma},\boldsymbol{r}\rangle}\, d\boldsymbol{\sigma} = \imath\kappa \int_0^1 e^{\imath\kappa z\zeta}\, d\zeta = \frac{1}{z}(e^{\imath\kappa z} - 1)$$

$$\frac{1}{\pi} \int_{\chi=0}^{+\infty} \int_{\phi=0}^{2\pi} e^{-\chi^2 z}\, e^{\imath\sqrt{\chi^4+\kappa^2}(x\cos\phi + y\sin\phi)}\, \chi\, d\chi\, d\phi = \int_0^{+\infty} e^{-\nu z}\, d\nu = \frac{1}{z}$$

Their sum is equal to $\frac{e^{\imath\kappa z}}{z}$, as expected. The integrand for the first integral is a smooth and oscillating function while the second integral contains the singularity for $|\boldsymbol{x}| \to 0$.

The new formula is formally similar to Eq. (1.1). However it has the considerable advantage of involving only functions which are well-behaved. Instead of one transfer function as before (see Eq. (1.2)), we have two transfer functions defined as:

$$T_{\boldsymbol{\sigma}}(\boldsymbol{r}) = \frac{\imath\kappa}{2\pi}\, e^{\imath\kappa\langle\boldsymbol{\sigma},\boldsymbol{r}\rangle}\, \mathbf{1}_{S^{z+}}(\boldsymbol{\sigma})$$

$$T^e_{\chi,\phi}(\boldsymbol{r}) = \frac{1}{\pi}\, \chi\, e^{-\chi^2 z}\, e^{\imath\sqrt{\chi^4+\kappa^2}(x\cos\phi + y\sin\phi)}\, \mathbf{1}_{[0:+\infty]}(\chi)$$

where $\mathbf{1}_{S^{z+}}$ is the characteristic function of the set S^{z+}, i.e.

$$\mathbf{1}_{S^{z+}}(\boldsymbol{\sigma}) = \begin{cases} 1 & \text{if } \boldsymbol{\sigma} \in S^{z+} \\ 0 & \text{if } \boldsymbol{\sigma} \notin S^{z+} \end{cases}$$

and $\mathbf{1}_{[0:+\infty]}(\chi)$ is the characteristic function of the set $[0 : +\infty]$ for χ.

This plane-wave expansion has been used previously by L. Greengard *et al.* (1998).

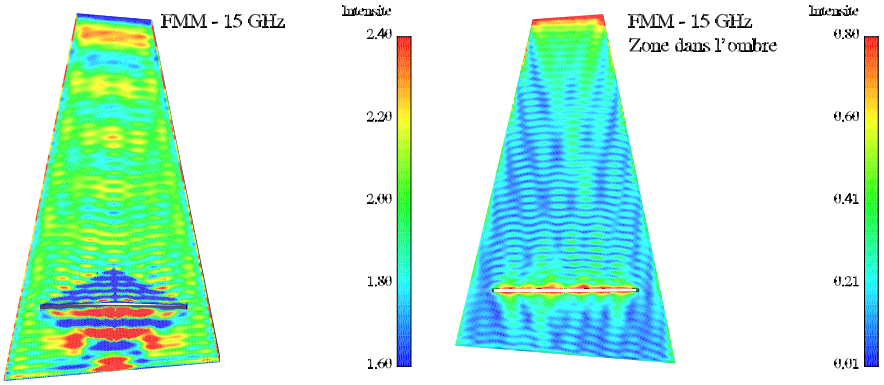

FIGURE 1. Example of an electromagnetics computation using the FMM. The code CEM3D was developed by E. Darve while at Paris 6 University. The geometry of the object was provided by Aerospatiale.

However their method is different from ours. In particular, it requires transformation operators to go from a traditional multipole expansion to a plane-wave expansion and vice-versa. In the opinion of the author, our new derivation is more consistent and conceptually simpler as we use only one kind of expansion, the plane-wave expansion. The FMM described in Greengard *et al.* involves steps with complexity p^3 where p^2 is the number of terms in the multipole expansion for a given cluster. In contrast, all operations for PW-FMM have complexity p^2.

The PW-FMM can also be used for $1/|\boldsymbol{r}|$ by setting $\kappa = 0$ in Eq. (1.3). This leads to the following expansion:

$$\frac{1}{|\boldsymbol{r}|} = \frac{1}{\pi} \int_{\chi=0}^{+\infty} \int_{\phi=0}^{2\pi} e^{-\chi^2 z}\, e^{\imath\chi^2(x\cos\phi + y\sin\phi)}\, \chi\, d\chi\, d\phi \tag{1.4}$$

The techniques presented in this article can thus be readily applied to $1/|\boldsymbol{r}|$ (Laplace equation, particle simulations, etc.).

We start this article by pointing out the limitations of the FMM for Maxwell and Helmholtz equations, in particular the fact that it is unstable at low frequency (Section 2). Then we describe our new technique, PW-FMM (Section 3), starting with the first term in the expansion (1.3) (Section 3.1) and ending with a description of the second term (Section 3.2).

2. Fast Multipole Method for electrodynamics scattering problems

To justify the need for a new method we start by describing the limitations of the traditional FMM for Maxwell/Helmholtz or high frequency FMM (HF-FMM) as we will call it from now on. The reasons for this name will become apparent in the next section.

2.1. *Numerical instabilities*

The HF-FMM has been successfully used in many large scale applications, for example by Song *et al.* (1997), Chew *et al.* (1997), Song *et al.* 1998, Darve (1999) and Darve (2000). Figures 1 and 2 illustrate some of the computations done by Darve using the FMM for radar scattering problems.

However there are two cases for which large numerical instabilities limit the usefulness

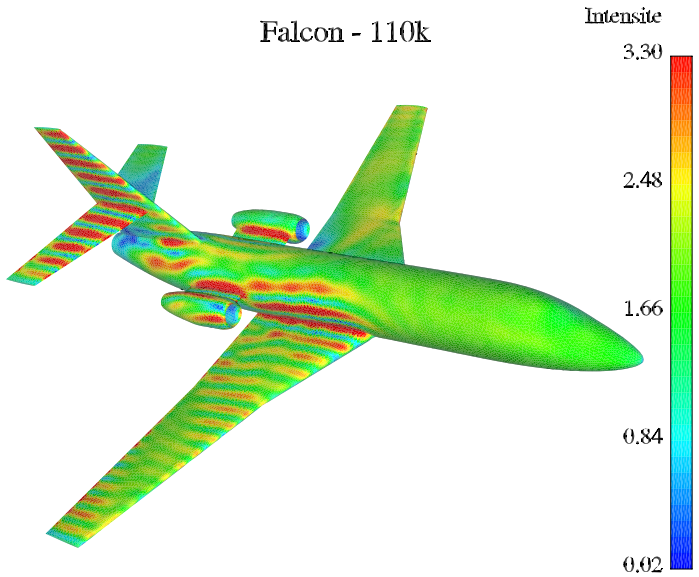

FIGURE 2. Example of an electromagnetics computation using the FMM. The code CEM3D was developed by E. Darve while at Paris 6 University. The geometry of the airplane was provided by Dassault-Aviation.

of the FMM. Let us consider the transfer function defined by Eq. (1.2). The asymptotic behavior of $h_m^{(1)}(x)$ is

$$|h_m^{(1)}(x)| \sim \begin{cases} \sqrt{\frac{2}{e}}\Big(\frac{2m+1}{e}\Big)^m \frac{1}{|x|^{m+1}} & \text{for } m \to +\infty \\ \frac{1\cdot 3\cdot 5\ldots(2m-1)}{|x|^{m+1}} & \text{for } x \to 0 \end{cases} \tag{2.1}$$

The numerical instabilities are caused by the divergence of $h_m^{(1)}(x)$ when $m \to +\infty$ or $x \to 0$.

In the FMM for electromagnetic scattering, the size of the smallest clusters is chosen so that the number of floating-point operations is of order $n \log n$. This is done by optimizing with respect to the computational expense of the far away interactions (approximated using the HF-FMM) and of the close interactions (exact evaluation). In particular, if the density of the points on the surface of the scattering object is increased, optimal complexity is achieved by reducing the size of the smallest clusters. If z_1 and z_2 are the centers of two clusters, $|\boldsymbol{z}_1 - \boldsymbol{z}_2|$ is proportional to the size of the clusters. Numerical instabilities appear when $\kappa|\boldsymbol{z}_1 - \boldsymbol{z}_2|$ becomes too small. Once $\kappa|\boldsymbol{z}_1 - \boldsymbol{z}_2| \ll m$, the function $h_m^{(1)}(\kappa|\boldsymbol{z}_1 - \boldsymbol{z}_2|)$ diverges (see Eq. (2.1)). This means that the transfer function $T_{l,z}(\boldsymbol{\sigma})$ diverges once $\kappa|\boldsymbol{z}_1 - \boldsymbol{z}_2| \ll l$. When implemented on a computer, this divergence causes large numerical instabilities because of roundoff errors.

The maximum density of points is large for very inhomogeneous distributions of points, or for low-frequency scattering when the diameter of the scattering object is very small compared to the wavelength (see Fig. 3). In these two cases, the numerical instabilities

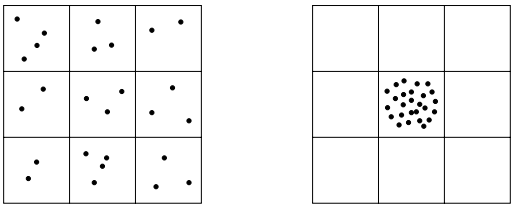

FIGURE 3. In the case of low-frequency scattering, the asymptotic complexity of the FMM is no longer of order $n \log n$. Suppose that ρ is the largest size of a cluster below which the computation is unstable. When the diameter of the object is smaller than ρ, the FMM consists of a single cluster containing all the points. All interactions have to be computed in a direct manner, without the use of the FMM. Then the complexity is on the order of n^2 rather than $n \log n$.

are so large that the FMM can no longer be used. Note that this behavior is very different from the behavior of the FMM for $1/r$ for which there is no such limitation.

The purpose of our new method is to remove this limitation on the size of the clusters. This guarantees a complexity in $n \log n$ for any distribution of points even if this distribution is very inhomogeneous.

Numerical instabilities can also appear when the error ϵ is smaller than some threshold. We know that ϵ for HF-FMM is, among other things, a function of l. More precisely a smaller ϵ requires a larger l. Considering Eq. (2.1), we see that $h_m^{(1)}(\kappa|\boldsymbol{z}_1 - \boldsymbol{z}_2|)$ starts to diverge if m becomes larger than $\kappa|\boldsymbol{z}_1 - \boldsymbol{z}_2|$. Thus if we decrease the tolerance criterion ϵ in HF-FMM below a certain threshold, the function $T_{l,z}(\boldsymbol{\sigma})$ diverges and again roundoff errors lead to numerical instabilities.

As a conclusion, even though the algorithm is well-behaved analytically, strong numerical instabilities prevent the use of HF-FMM for low frequency applications and high accuracy computations.

2.2. *Comparison with other variants of the FMM*

Numerous authors, such as Greengard *et al.* (1998), Hu *et al.* (1999) and Hu & Chew (1999), have devised algorithms to tackle this problem. However these algorithms are not entirely satisfactory. The low-frequency Fast Multipole Method (LF-FMM) of Greengard and Rokhlin (1987) is a very complex scheme and requires complex transformations from multipole expansions to plane wave expansions and vice-versa. The Fast Inhomogeneous Plane Wave Expansion method of Hu *et al.* (1999) has the disadvantage of lacking a clear mathematical foundation, and several theoretical issues have not been satisfactorily settled. In particular, error and rates of convergence have not been well estimated so far.

We propose a new method, called Plane Wave Fast Multipole Method (PW-FMM) which is based on plane wave expansions. It is related to Rokhlin-Greengard's and Hu-Chew's techniques. However, it has the advantage of being simpler and more efficient and precise error estimations can be derived.

Unlike HF-FMM, PW-FMM is stable at all frequencies and any accuracy can be achieved with this method. Moreover we will show that for high-frequency applications the number of floating-point operations is less in PW-FMM.

3. Plane Wave Fast Multipole Method

Vectors are denoted using bold face, e.g. $\boldsymbol{v}$. Integers are denoted using Latin letters, e.g. n, while real numbers are denoted using Greek letters, e.g. λ.

The PW-FMM is based on the following expansion:

$$\frac{e^{\imath\kappa|\boldsymbol{r}|}}{|\boldsymbol{r}|} = \frac{\imath\kappa}{2\pi}\int_{S^{z+}} e^{\imath\kappa\langle\boldsymbol{\sigma},\boldsymbol{r}\rangle}\, d\boldsymbol{\sigma} + \frac{1}{\pi}\int_{\chi=0}^{+\infty}\int_{\phi=0}^{2\pi} e^{-\chi^2 z}\, e^{\imath\sqrt{\chi^4+\kappa^2}(x\cos\phi+y\sin\phi)}\, \chi\, d\chi\, d\phi \quad (3.1)$$

where $\boldsymbol{r} = (x, y, z)$. The set S^{z+} is the subset of S^2 of all the points with positive z-coordinate:

$$S^{z+} = \{\boldsymbol{\sigma} = (x, y, z),\ |\boldsymbol{\sigma}| = 1, z > 0\}$$

The variable χ has dimension of the square root of a frequency. It can be readily seen that Eq. (3.1) is a good candidate for a fast multipole method. Indeed if discretization points $\boldsymbol{\sigma}_q$ and $\boldsymbol{\sigma}_q^e$ and weights ω_q and ω_q^e are chosen, Eq. (3.1) can be written in the following manner:

$$\begin{aligned}\frac{e^{\imath\kappa|\boldsymbol{x}_i-\boldsymbol{x}_j|}}{|\boldsymbol{x}_i-\boldsymbol{x}_j|} \sim &\sum_q \omega_q\, T_{\sigma_q}(\boldsymbol{z}_1-\boldsymbol{z}_2)\, f_{\sigma_q}(\boldsymbol{x}_i-\boldsymbol{z}_1) f_{\sigma_q}(\boldsymbol{z}_2-\boldsymbol{x}_j)\\ &+\sum_q \omega_q^e\, T^e_{\sigma_q^e}(\boldsymbol{z}_1-\boldsymbol{z}_2)\, f^e_{\sigma_q^e}(\boldsymbol{x}_i-\boldsymbol{z}_1) f^e_{\sigma_q^e}(\boldsymbol{z}_2-\boldsymbol{x}_j)\end{aligned}$$

with

$$\begin{aligned}\boldsymbol{\sigma}_q &= (\sin\theta_q\cos\phi_q, \sin\theta_q\sin\phi_q, \cos\theta_q)\\ T_\sigma(\boldsymbol{z}) &= \exp(\imath\kappa\langle\boldsymbol{\sigma},\boldsymbol{z}\rangle)\\ f_\sigma(\boldsymbol{x}) &= T_\sigma(\boldsymbol{x})\end{aligned}$$

and

$$\begin{aligned}\boldsymbol{\sigma}_q^e &= (\chi_q, \phi_q)\\ T^e_\sigma(\boldsymbol{z}) &= \chi\ \exp(-\chi^2\boldsymbol{z}_z)\ \exp(\imath\sqrt{\chi^4+\kappa^2}(\boldsymbol{z}_x\cos\phi+\boldsymbol{z}_y\sin\phi))\\ f^e_\sigma(\boldsymbol{x}) &= \exp(-\chi^2\boldsymbol{x}_z)\ \exp(\imath\sqrt{\chi^4+\kappa^2}(\boldsymbol{x}_x\cos\phi+\boldsymbol{x}_y\sin\phi))\end{aligned}$$

Bold face is used for 3D points while an index in normal face x, y, or z designate the x, y, or z coordinate of a point. The new basis functions for PW-FMM can be used in exactly the same manner as for HF-FMM. We now describe in more detail the behavior of the basis functions in Fourier space, and more specifically the fact that they are band-limited in Fourier space.

We define:

- Propagating term : $\int_{S^{z+}} e^{\imath\kappa\langle\boldsymbol{\sigma},\boldsymbol{x}\rangle}\, d\boldsymbol{\sigma}$.
- Evanescent term : $1/\pi\int_{\chi=0}^{+\infty}\int_{\phi=0}^{2\pi} e^{-\chi^2\boldsymbol{x}_z}\, e^{\imath\sqrt{\chi^4+\kappa^2}(\boldsymbol{x}_x\cos\phi+\boldsymbol{x}_y\sin\phi)}\, \chi\, d\chi\, d\phi$.

3.1. *Propagating term*

The propagating term is the simplest of the two terms. It is almost identical to the basis function for HF-FMM. However there is a significant fact which must be recognized.

In the Multipole to Multipole step of the FMM we proceed as usual. The functions f_{C_k} are computed as:

$$f_{C_k}(\boldsymbol{\sigma}_q) = \sum_{\boldsymbol{x}_i\in C_k} u_i\, e^{\imath\kappa\langle\boldsymbol{\sigma}_q,\boldsymbol{x}_i-\boldsymbol{z}_k\rangle} \quad (3.2)$$

Then, in the Multipole to Local step, the functions g_{C_k} are computed as:

$$g_{C_k}(\boldsymbol{\sigma}_q) = \sum_r e^{\imath\kappa\langle\boldsymbol{\sigma}_q,\boldsymbol{z}_k-\boldsymbol{z}_r\rangle}\ f_{C_r}(\boldsymbol{\sigma}_q)$$

However at this point some care must be taken. One may think that the usual interpolation can be performed for Local to Local transformations. However, the final integration is over S^{z+} only, so that the integration is actually:

$$\int_{S^{z+}} e^{\imath\kappa\langle\boldsymbol{\sigma},\boldsymbol{z}_r-\boldsymbol{x}_j\rangle} g_{C_k}(\boldsymbol{\sigma})\,d\boldsymbol{\sigma} = \int_{S^2} \left\{ e^{\imath\kappa\langle\boldsymbol{\sigma},\boldsymbol{z}_r-\boldsymbol{x}_j\rangle} \mathbf{1}_{S^{z+}}(\boldsymbol{\sigma}) \right\} g_{C_k}(\boldsymbol{\sigma})\,d\boldsymbol{\sigma}$$

An efficient implementation of the FMM requires that we can efficiently Fourier-transform band-limited functions, and these transforms are defined on S^2 rather than S^{z+}. The function $e^{\imath\kappa\langle\boldsymbol{\sigma},\boldsymbol{z}_r-\boldsymbol{x}_j\rangle}\mathbf{1}_{S^{z+}}(\boldsymbol{\sigma})$ has a very slowly decaying Fourier spectrum because of the discontinuity. As a consequence, the number of sample points on S^2 will be very large. This approach does not lead to an $n \log n$ method and therefore is not good.

The solution consists in moving the characteristic function to the transfer function. We define the transfer function as

$$T_\sigma(\boldsymbol{z}_k - \boldsymbol{z}_r) = \mathbf{1}_{S^{z+}}(\boldsymbol{\sigma})\; e^{\imath\kappa\langle\boldsymbol{\sigma},\boldsymbol{z}_k-\boldsymbol{z}_r\rangle}$$

Now the functions g_{C_k} are defined as:

$$g_{C_k}(\boldsymbol{\sigma}) = \sum_r \mathbf{1}_{S^{z+}}(\boldsymbol{\sigma})\; e^{\imath\kappa\langle\boldsymbol{\sigma},\boldsymbol{z}_k-\boldsymbol{z}_r\rangle}\; f_{C_r}(\boldsymbol{\sigma})$$

and the final integration is:

$$\int_{S^2} e^{\imath\kappa\langle\boldsymbol{\sigma},\boldsymbol{z}_r-\boldsymbol{x}_j\rangle}\; g_{C_k}(\boldsymbol{\sigma})\,d\boldsymbol{\sigma}$$

In Darve (1999), it is shown that $e^{\imath\kappa\langle\boldsymbol{\sigma},\boldsymbol{z}_r-\boldsymbol{x}_j\rangle}$ has a bandwidth on the order of $\kappa|\boldsymbol{z}_r-\boldsymbol{x}_j|$. The functions $f_{C_r}(\boldsymbol{\sigma}_q)$ have a bandwidth of the same order, more precisely $\kappa \max|\boldsymbol{x}_i-\boldsymbol{z}_k|$ (see Eq. (3.2)). Thus we can retain only the first $\kappa(|\boldsymbol{z}_r-\boldsymbol{x}_j|+\max|\boldsymbol{x}_i-\boldsymbol{z}_k|)$ frequencies in $T_\sigma(\boldsymbol{z}_k-\boldsymbol{z}_r)$. If we denote by ρ the length of the side of the cubic clusters, then

$$\kappa|\boldsymbol{z}_r-\boldsymbol{x}_j| \le \kappa\rho \qquad \kappa\max|\boldsymbol{x}_i-\boldsymbol{z}_k| \le \kappa\rho$$

Thus we need on the order of $2\kappa\rho$ frequencies for $T_\sigma(\boldsymbol{z}_k-\boldsymbol{z}_r)$. To obtain the most efficient form of the FMM it is crucial always to retain the minimal number of frequencies, as this will affect the number of sample points required on the unit sphere.

Numerical tests of accuracy must be made to find the precise relation between the tolerance criterion ϵ and the exact number of frequencies that need to be retained. T is constructed in the following manner:

PROCEDURE 1 (CONSTRUCTION OF T). *We describe the construction of T for the propagating term when a transfer is to be performed in the direction $+z$. First we need to find the minimum number of frequencies l needed for $T_\sigma(\boldsymbol{z}_k-\boldsymbol{z}_r)$ for a given accuracy ϵ. This number is on the order of $2\kappa\rho$ where ρ is the size of a cluster. Then we Fourier-transform*

$$\mathbf{1}_{S^{z+}}(\boldsymbol{\sigma})\; e^{\imath\kappa\langle\boldsymbol{\sigma},\boldsymbol{z}_k-\boldsymbol{z}_r\rangle},$$

retain only the first l frequencies and inverse-Fourier-transform our function to obtain $T_\sigma(\boldsymbol{z}_k-\boldsymbol{z}_r)$. We now have a transfer function with the minimal number of frequencies and thus the minimal number of sample points for a given error ϵ.

For all other directions $z-$, $x\pm$ and $y\pm$, the same construction applies. This defines the transfer functions for all possible directions.

We did some numerical tests to illustrate this construction. Consider the following

function:

$$f_C(\theta,\phi) = \sum_{i=1}^{10} u_i \, e^{\imath\langle(\theta,\phi),\boldsymbol{x}_i\rangle}$$

where $\boldsymbol{x}_i$ are random points inside a sphere of radius 16, and u_i are random coefficients. We compute:

$$\int_{\theta=-\pi/2}^{\pi/2} f_C(\theta,0)\, e^{\imath\langle(\theta,0),\boldsymbol{z}\rangle}\, d\theta \tag{3.3}$$

where $\boldsymbol{z}$ is equal to $(32,32,64)$. We now denote

$$T_\infty(\theta) = e^{\imath\langle(\theta,0),\boldsymbol{z}\rangle}\mathbf{1}_{[-\pi/2:\pi/2]}(\theta)$$

We wish to show that using Procedure 1 for $T_\infty(\theta)$ allows accurately computing integral (3.3) with a relatively small number of sample points for $f_C(\theta,0)$. Procedure 1 is applied in the following way. We Fourier transform $T_\infty(\theta)$, retain the lowest p frequencies, and set the higher frequencies to zero. Then we take the inverse Fourier transform. Let us denote the resulting function by T_p. We then approximate integral (3.3) using:

$$\frac{2\pi}{2p+1}\sum_{q=1}^{2p+1} f_C(\frac{2\pi q}{2p+1},0)\; T_p(\frac{2\pi q}{2p+1})$$

We proved that the bandwidth of $f_C(\theta,0)$ in θ is on the order of the radius of the sphere, 16. Thus we expect a very fast convergence once p is larger than 32. Figure 4 shows that this is indeed the case. Consider the case with 64 sample points: at this resolution the error is down to 1.7×10^{-9}, so the computation is very accurate. This corresponds to a case where the transfer function $T_\infty(\theta)$ is under-resolved. The number of sample points 64 is too small to resolve the high frequencies of the function. Figure 5 represents the exact transfer function $T_\infty(\theta)$ and the low-frequency approximate T_p that is used for $p=64$. However since $f_C(\theta,0)$ is band limited and its bandwidth is on the order of 16, the computation is accurate if we use T_p rather than T_∞. It may seem paradoxical that increased accuracy is achieved by modifying the function $T_\infty(\theta)$. The argument is that since $f_C(\theta,0)$ is band limited, the contribution of any frequency in $T_\infty(\theta)$ that is higher than 16 in this case is negligible. However since we only use 64 sample points for the discrete approximation of the integral, these high frequencies contribute. By smoothing $T_\infty(\theta)$ we exactly remove any contribution from the high frequencies and thus improve the accuracy.

3.2. *Evanescent term*

Consider two points $\boldsymbol{x}_i$ in cluster C_1 with center $\boldsymbol{z}_1$, and $\boldsymbol{x}_j$ in cluster C_2 with center $\boldsymbol{z}_2$. We have the following expansion:

$$\begin{aligned}\frac{e^{\imath\kappa|\boldsymbol{x}_i-\boldsymbol{x}_j|}}{|\boldsymbol{x}_i-\boldsymbol{x}_j|} =& \frac{\imath\kappa}{2\pi}\int_{S^{z+}} e^{\imath\kappa\langle\boldsymbol{\sigma},\boldsymbol{x}_i-\boldsymbol{x}_j\rangle}\, d\boldsymbol{\sigma} \\ &+ \frac{1}{\pi}\int_{\chi=0}^{+\infty}\int_{\phi=0}^{2\pi} e^{-\chi^2(\boldsymbol{x}_i-\boldsymbol{x}_j)_z}\; e^{\imath\sqrt{\chi^4+\kappa^2}((\boldsymbol{x}_i-\boldsymbol{x}_j)_x\cos\phi+(\boldsymbol{x}_i-\boldsymbol{x}_j)_y\sin\phi)}\; \chi\, d\chi\, d\phi\end{aligned}$$

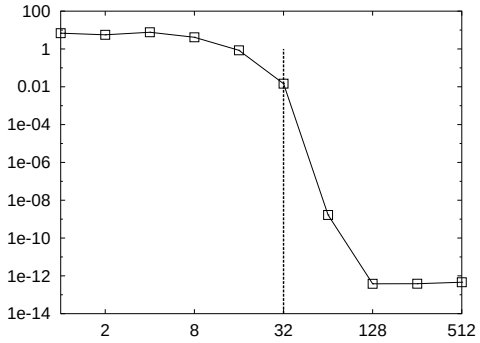

FIGURE 4. The figure represents the decrease of the error with the number of sample points for the computation of $\int_{\theta=-\pi/2}^{\pi/2} f_C(\theta,0)\, e^{\imath\langle(\theta,0),\boldsymbol{z}\rangle}\, d\theta$. The vertical thick line | is located at 32. Once the number of sample points is larger than the diameter of the sphere (32 in this case) the convergence is very fast.

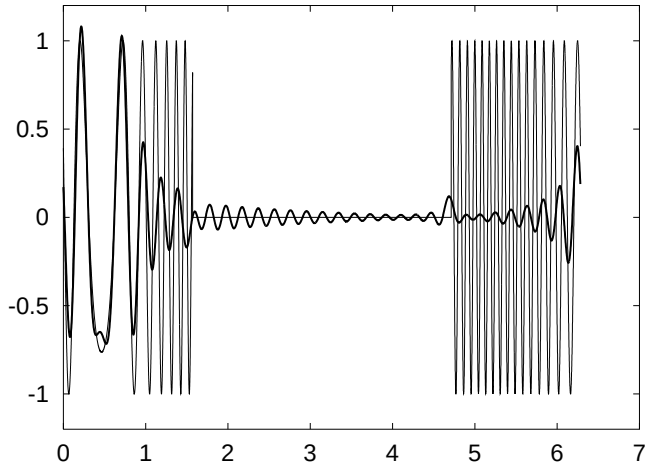

FIGURE 5. This figure compares the function $T_\infty(\theta)$ (thin line —) with the smooth function T_p (thick line —) used in the integration.

The integrand for the evanescent term can be split into three functions:

$$F_{\boldsymbol{x}_i-\boldsymbol{z}_1}(\chi,\phi) = e^{-\chi^2(\boldsymbol{x}_i-\boldsymbol{z}_1)_z}\; e^{\imath\sqrt{\chi^4+\kappa^2}((\boldsymbol{x}_i-\boldsymbol{z}_1)_x\cos\phi+(\boldsymbol{x}_i-\boldsymbol{z}_1)_y\sin\phi)}$$

$$T_{\boldsymbol{z}_1-\boldsymbol{z}_2}(\chi,\phi) = \mathbf{1}_{[0:+\infty]}(\chi)\;\chi\; e^{-\chi^2(\boldsymbol{z}_1-\boldsymbol{z}_2)_z}\; e^{\imath\sqrt{\chi^4+\kappa^2}((\boldsymbol{z}_1-\boldsymbol{z}_2)_x\cos\phi+(\boldsymbol{z}_1-\boldsymbol{z}_2)_y\sin\phi)}$$

$$G_{\boldsymbol{z}_2-\boldsymbol{x}_j}(\chi,\phi) = e^{-\chi^2(\boldsymbol{z}_2-\boldsymbol{x}_j)_z}\; e^{\imath\sqrt{\chi^4+\kappa^2}((\boldsymbol{z}_2-\boldsymbol{x}_j)_x\cos\phi+(\boldsymbol{z}_2-\boldsymbol{x}_j)_y\sin\phi)}$$

The evanescent term is now equal to:

$$\mathcal{I}(\boldsymbol{x}_i-\boldsymbol{x}_j) = \frac{1}{\pi}\int_{\chi=-\infty}^{+\infty}\int_{\phi=0}^{2\pi} F_{\boldsymbol{x}_i-\boldsymbol{z}_1}(\chi,\phi)\, T_{\boldsymbol{z}_1-\boldsymbol{z}_2}(\chi,\phi)\, G_{\boldsymbol{z}_2-\boldsymbol{x}_j}(\chi,\phi)\;\chi\, d\chi\, d\phi. \qquad (3.4)$$

In order to reduce the number of sample points χ and ϕ, the functions $F_{\boldsymbol{x}_i-\boldsymbol{z}_1}$ and $G_{\boldsymbol{z}_2-\boldsymbol{x}_j}$ need to be band limited in Fourier space for the variables χ and ϕ. For the variable χ, this condition is not true, as $(\boldsymbol{x}_i-\boldsymbol{z}_1)_z$ and $(\boldsymbol{z}_2-\boldsymbol{x}_j)_z$ can have either sign and thus

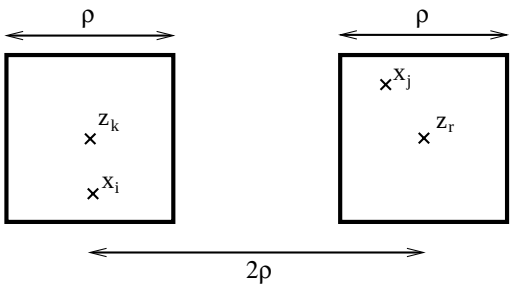

FIGURE 6. Size and distance between clusters. ρ is the length of the side of the clusters and 2ρ is the minimal distance between two clusters which are not neighbors.

$e^{-\chi^2(\boldsymbol{x}_i-\boldsymbol{z}_1)_z}$ and $e^{-\chi^2(\boldsymbol{z}_2-\boldsymbol{x}_j)_z}$ may be diverging exponentials. However $(\boldsymbol{x}_i-\boldsymbol{z}_1)_z$ and $(\boldsymbol{z}_2-\boldsymbol{x}_j)_z$ satisfy the following equations, where ρ is the size of clusters C_1 and C_2 (see Fig. 6):

$$(\boldsymbol{x}_i-\boldsymbol{z}_1)_z \geq \frac{-\rho}{2}, \tag{3.5}$$

$$(\boldsymbol{z}_2-\boldsymbol{x}_j)_z \geq \frac{-\rho}{2}, \tag{3.6}$$

$$(\boldsymbol{z}_1-\boldsymbol{z}_2)_z \geq 2\rho. \tag{3.7}$$

Suppose we multiply $F_{\boldsymbol{x}_i-\boldsymbol{z}_1}(\chi,\phi)$, $G_{\boldsymbol{z}_2-\boldsymbol{x}_j}(\chi,\phi)$ and $T_{\boldsymbol{z}_1-\boldsymbol{z}_2}(\chi,\phi)$ by the following factors:

$$\tilde{F}_{\boldsymbol{x}_i-\boldsymbol{z}_1}(\chi,\phi) \stackrel{\text{def}}{=} \exp(-\chi^2\frac{3\rho}{4})\, F_{\boldsymbol{x}_i-\boldsymbol{z}_1}(\chi,\phi) \tag{3.8}$$

$$\tilde{T}_{\boldsymbol{z}_1-\boldsymbol{z}_2}(\chi,\phi) \stackrel{\text{def}}{=} \exp(\chi^2\frac{3\rho}{2})\, T_{\boldsymbol{z}_1-\boldsymbol{z}_2}(\chi,\phi) \tag{3.9}$$

$$\tilde{G}_{\boldsymbol{z}_2-\boldsymbol{x}_j}(\chi,\phi) \stackrel{\text{def}}{=} \exp(-\chi^2\frac{3\rho}{4})\, G_{\boldsymbol{z}_2-\boldsymbol{x}_j}(\chi,\phi) \tag{3.10}$$

then the functions $\tilde{F}_{\boldsymbol{x}_i-\boldsymbol{z}_1}(\chi,\phi)$ and $\tilde{G}_{\boldsymbol{z}_2-\boldsymbol{x}_j}(\chi,\phi)$ are band limited for χ. The factors were chosen so that the decay, when χ goes to infinity, of

$$\tilde{F}_{\boldsymbol{x}_i-\boldsymbol{z}_1}(\chi,\phi)\,\tilde{G}_{\boldsymbol{z}_2-\boldsymbol{x}_j}(\chi,\phi)$$

is similar to the decay of $\tilde{T}_{\boldsymbol{z}_1-\boldsymbol{z}_2}(\chi,\phi)$. More precisely, we have the following bounds:

$$|\tilde{T}_{\boldsymbol{z}_1-\boldsymbol{z}_2}(\chi,\phi)| \leq |\chi|\ \exp(-\chi^2\frac{\rho}{2})$$

$$|\tilde{F}_{\boldsymbol{x}_i-\boldsymbol{z}_1}(\chi,\phi)\,\tilde{G}_{\boldsymbol{z}_2-\boldsymbol{x}_j}(\chi,\phi)| \leq \exp(-\chi^2\frac{\rho}{2})$$

A procedure similar to Procedure 1 can be used to construct $T^e_{\boldsymbol{z}_1-\boldsymbol{z}_2}$ from $\tilde{T}_{\boldsymbol{z}_1-\boldsymbol{z}_2}$.

We do not detail the implementation and sampling procedure for variables ϕ and χ. It is similar to the construction of Section 3.1 and is based on studying the decay of the Fourier spectrum of f_{C_k} for ϕ and χ.

4. Conclusion

The new scheme presented in this article is based on plane-wave expansion. Unlike previous formulations, it is stable at all frequencies and is more accurate. This Plane

Wave FMM (PW-FMM) involves a decomposition of $\exp(\imath kr)/r$ using two kinds of plane waves: evanescent and propagating. The basic tools required for PW-FMM are similar to the traditional FMM formulation (HF-FMM), but PW-FMM is stable at all frequencies and more accurate than HF-FMM.

Stability at all frequencies allows PW-FMM to be used as an adaptive method, i.e. it is possible to consider adaptive trees, where the number of levels varies depending on the concentration of points. For scattering applications, this means that the method remains efficient even if tiny details of the surface need to be meshed using a large number of points concentrated in a small volume. This is not possible with HF-FMM because of the sub-wavelength "breakdown".

A future publication will present the implementation of PW-FMM, a precise description of the various optimization steps which can be performed, and some numerical results. In particular, it will contain an analysis of the performance of the method and its accuracy.

REFERENCES

Cheng, H., Greengard, L. & Rokhlin, V. 1999 A fast adaptive multipole algorithm in three dimensions. *J. Comp. Phys.* **155**, 468-498.

Chew, W. C., Jin, J. M., Lu, C. C., Michielssen, E. & Song, J. M. 1997 Fast solution methods in electromagnetics. *IEEE Trans. on Anten. and Propa.* **45**, 533-543.

Darve, E. 1997 Fast-multipole: a mathematical study (abridged version). *C. R. Acad. Sci. Paris*, **Série I**, 1037-1042.

Darve, E. 1999 *Méthodes multipôles rapides: résolution des équations de Maxwell par formulations intégrales.* Ph.D. in Applied Math., Université Pierre et Marie Curie, Paris.

Darve, E. 1999 The fast multipole method (i): error analysis and asymptotic complexity. *SIAM J. Num. Anal.* **38**, 98-128.

Darve, E. 2000 The fast multipole method: numerical implementation. *J. Comp. Phys.* **160**, 195-240.

Engheta, N., Murphy, W. D., Rokhlin, V. & Vassiliou, M. S. 1992 The fast multipole method (FMM) for electromagnetic scattering problems. *IEEE Trans. on Anten. and Propa.* **40**, 634-641.

Epton, M. A. & Dembart, B. 1995 Multipole translation theory for three-dimensional laplace and helmholtz equations. *SIAM J. Sci. Comput.* **16**, 865-897.

Greengard, L. & Rokhlin, V. A fast algorithm for particle simulations. *J. Comp. Phys.* **73**, 325-348.

Greengard, L., Huang, J., Rokhlin, V. & Wandzura, S. 1998 Accelerating fast multipole methods for low frequency scattering. *IEEE Comp. Sci. & Engineering Mag.* **5**, 32-38.

Hu, B. & Chew, W. C. 1999 Fast inhomogeneous plane wave algorithm for electromagnetic solutions in layered medium structures. In *36th Ann. Tech. Mtg., Soc. of Engg. Sci.*, Austin, Texas.

Hu, B., Chew, W. C., Michielssen, E. & Zhao, J. 1999 Fast inhomogeneous plane wave algorithm (FIPWA) for the fast analysis of two-dimensional scattering problems. University of Illinois, Urbana, *Research Report* CCEM-5-99.

Rokhlin, V. 1990 Rapid solution of integral equations of scattering theory in two dimensions. *J. Comp. Phys.* **86**, 414-439.

Song, J. M., Lu, C. C. & Chew, W. C. 1997 Multilevel fast multipole algorithm for electromagnetic scattering by large complex objects. *IEEE Trans. on Anten. and Propag.* **45**, 1488-1493.

Song, J. M., Lu, C. C., Chew, W. C. & Lee, S. W. 1998 Fast illinois solver code (FISC). *IEEE Anten. and Propag. Mag.* **40**, 27-33.

White, C. A. & Headgordon, M. 1996 Rotating around the quartic angular-momentum barrier in fast multipole method calculations. *J. Chem. Phys.* **105**, 5061-5067.